View metadata, citation and similar papers at core.ac.uk

brought to you by CORE

provided by NASA Technical Reports Server

INFRARED-ULTRAVIOLET SPECTRA OF ACTIVE GALACTIC NUCLEI

M.A. Malkan
Department of Astronomy, University of California, Los Angeles

and

R.A. Edelson
Owens Valley Radio Observatory, California Institute of Technology

Data from IRAS and IUE were combined with ground-based optical and infrared spectrophotometry to derive emission-line-free spectral energy distributions (SEDs) for 29 active galactic nuclei (AGNs) between 0.1 and 100 μm. The IRAS data were scaled down to account for extended emission. These correction factors, determined by comparing small-aperture ground-based 10.6 μm data with large-aperture IRAS 12 μm fluxes, were usually less than 25%. These corrected SEDs are shown in Figure 1.

Although the contaminating effects of reddening and emission from stars and dust in the underlying galaxy are significant in some SEDs, they usually can be corrected adequately. Several good indicators of nuclear dust in AGNs are identified, all of which are well correlated: 1) Steepness of infrared spectral index; 2) Reddening derived from the shape of the ultraviolet continuum; 3) Strength of the 2200 Å dust absorption feature; 4) Line ratios, such as Hα/Hβ and Lyα/Hβ; and 5) Line-free continuum colors, such as f_{4220}/f_{1770} and f_{4220}/f_{1450}.

Dust does not play a major role in many of the Seyfert 1 galaxies and quasars in this sample. The SEDs of these objects are generally well described by a simple model consisting of four spectral components, each of which dominates over a different wavelength region. Figure 2 is a plot of the model fits to three AGNs, decomposed to show the individual components. The first, which usually contains most of the total luminosity between 0.1 and 100 μm, is a power-law with $\overline{\alpha_{pl}} = -1.36 \pm 0.21$ (RMS scatter for individual objects). This power-law often has a sharp low-frequency cut-off between 40 and 100 μm, and in most of the remaining objects, the SEDs are constrained to turn over by ~ 300 μm. The simplest explanation is that the infrared luminosity is dominated by synchrotron emission from a self-absorbed source a few hundred Schwarzschild radii across, about the size of the hypothesized accretion disk. There is a strong correlation between the luminosity from this power-law at 5450 Å and the 2 keV X-ray luminosity, which suggests that the power-law may extend at least from X-ray to far-infrared wavelengths (5 1/2 decades of frequency).

The second component, which was detected in over one-half the SEDs, was a broad near-infrared excess, described by a parabola centered at 5.2 μm, with a FWHM of 3.3 frequency octaves. Although it contains less total energy than the Balmer continuum, it can account for up to 40% of the total luminosity between 2.5 and 10 μm. Its strength is well correlated with total luminosity and Hβ/[O III] ratio.

The far-ultraviolet emission is dominated by a component which was described as a blackbody with T ~ 26,000 ± 4,000 K (individual scatter). The fitted Balmer

Carol J. Lonsdale Persson (Editor)
Star Formation in Galaxies

PRECEDING PAGE BLANK NOT FILMED

Figure 1 (a-d)

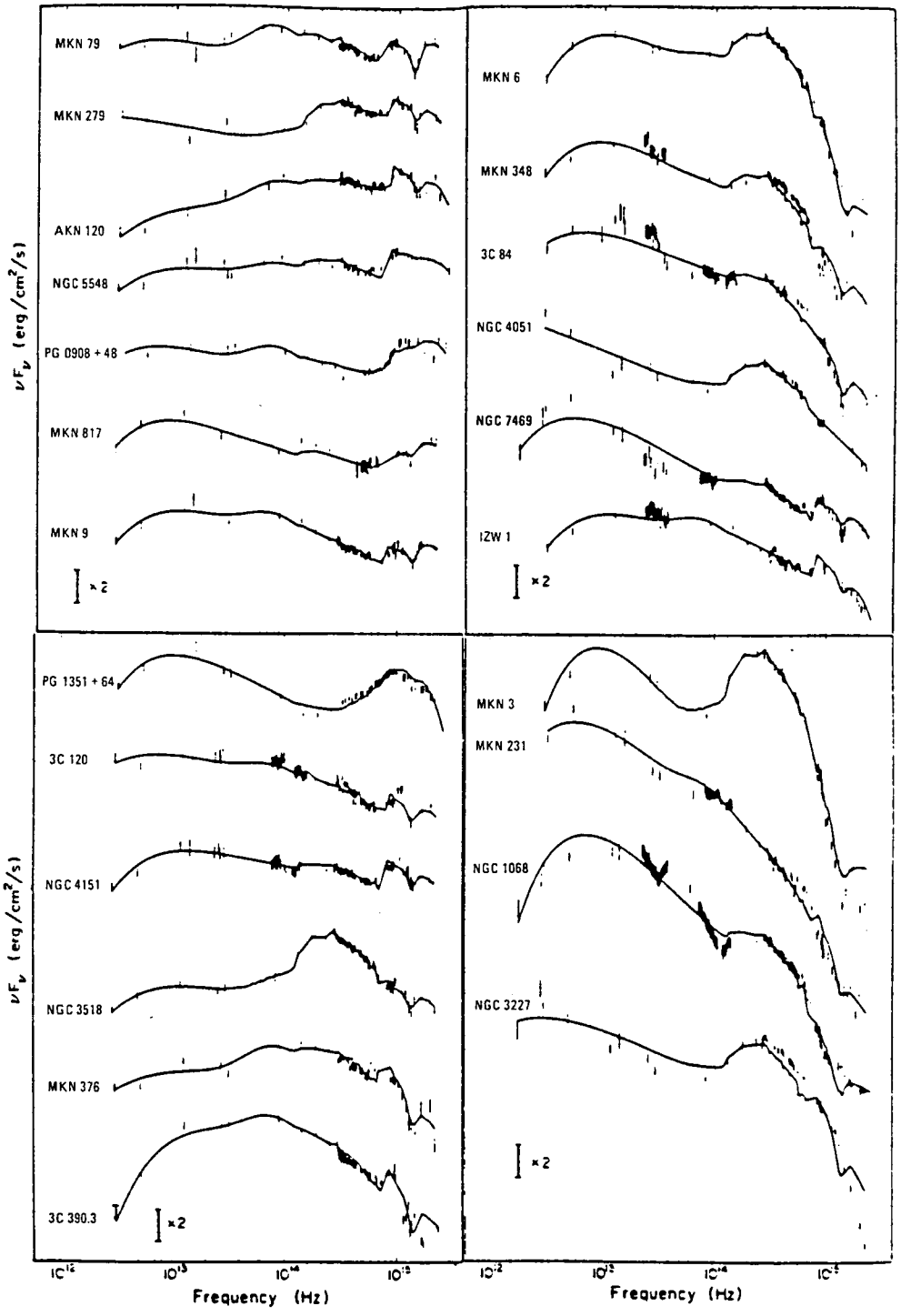

Figure 1. Fits to the infrared/optical/ultraviolet SEDs of 29 AGNs are presented in Figure 1. Observed binned continuum fluxes are shown with vertical error bars. The lines show the best-fitting models with a power law, near-infrared bump, and ultraviolet blackbody (including corrections for reddening, starlight and recombination radiation). Vertical scale is logarithm of νF_ν, so that a power-law of slope -1 (with equal power per decade) would appear as a horizontal line. The large vertical bar shows a factor of 2 in flux.

Figure 1 (e)

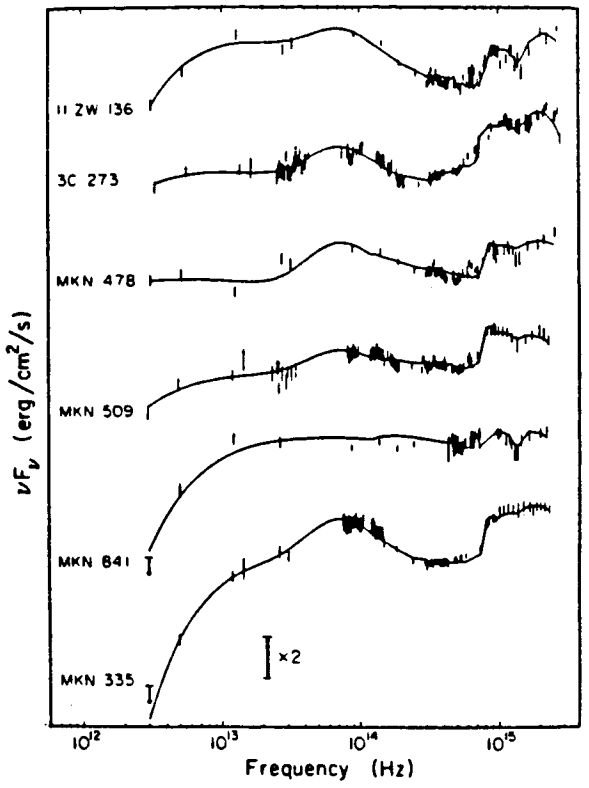

Figure 2

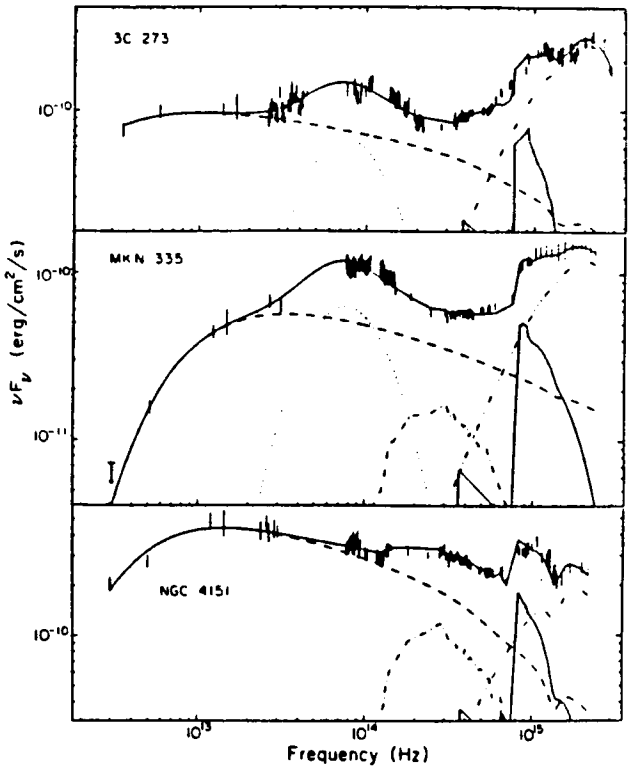

Figure 2. Detail of model fits to SEDs of 3C 273, Mkn 335, and NGC 4151. The individual components shown are the infrared power law (dashed line, which dominates the far-infrared), the near-infrared bump (dotted line; not detected in NGC 4151), the galactic starlight (dot-dash line, not detectable in 3C 273), the recombination continuum (solid line--only the Balmer continuum and a little of the Paschen continuum are strong enough to show in the figures), and the ultraviolet blackbody (dot-dot-dash line). All components have been reddened by galactic and internal reddening. The sum of these components equals the fitted model, shown by the upper solid line.

continuum/Hα ratio for the Seyfert 1 galaxies is 2.1 $\pm$ 0.6, under the assumption that the emission is optically thin with T_e = 13,000 K. This ratio is significantly greater than the prediction of Case B recombination, and shows no correlations with other AGN properties. Seyfert 2 galaxies have a lower Balmer continuum/Hα ratio than Seyfert 1 galaxies.

Although the power-law model fitted the relatively dust-free objects well, it failed to reproduce the SEDs of Seyfert 2 galaxies and Seyfert 1 galaxies with large reddenings and other strong dust indicators (i.e., NGC 3227, NGC 7469, and Mkn 231) because their fluxes beyond 10 μm are significantly contaminated by thermal emission from dust. They have minimum dust temperatures of 35-60 K, which is warmer than in normal spiral galaxies. The thermal emission appears to arise from ~ 100 $M_\odot$ of dust in a volume similar to that of the narrow line region. Low-luminosity active galaxies with 100 μm fluxes dominated by dust emission from the underlying galactic disk showed large differences between small-aperture ground-based 10-μm and large-aperture IRAS 12-μm fluxes, and steep spectral indices between 60 and 100 μm.